PAPER

Interfacial behavior of the decane + brine + surfactant system in the presence of carbon dioxide, methane, and their mixture†

Nilesh Choudhary, [ID] Arun Kumar Narayanan Nair [ID]* and Shuyu Sun*

Molecular dynamics simulations are carried out to get insights into the interfacial behavior of the decane + brine + surfactant + CH_4 + CO_2 system at reservoir conditions. Our results show that the addition of CH_4, CO_2, and sodium dodecyl sulfate (SDS) surfactant at the interface reduces the IFTs of the decane + water and decane + brine (NaCl) systems. Here the influence of methane was found to be less pronounced than that of carbon dioxide. As expected, the addition of salt increases the IFTs of the decane + water + surfactant and decane + water + surfactant + CH_4/CO_2 systems. The IFTs of these surfactant-containing systems decrease with temperature and the influence of pressure is found to be less pronounced. The atomic density profiles show that the sulfate head groups of the SDS molecules penetrate the water-rich phase and their alkyl tails are stretched into the decane-rich phase. The sodium counterions of the surfactant molecules are located very close to their head groups. Furthermore, the density profiles of water and salt ions are hardly affected by the presence of the SDS molecules. However, the interfacial thickness between water and decane/CH_4/CO_2 molecules increases with increasing surfactant concentration. An important result is that the enrichment of CH_4 and/or CO_2 in the interfacial region decreases with increasing surfactant concentration. These results may be useful in the context of the water-alternating-gas approach that has been utilized during CO_2-enhanced oil recovery operations.

1 Introduction

The emission of anthropogenic CO_2 is one of the major causes of global climatic changes.[1–4] Carbon capture and storage technology might be beneficial for mitigating these emissions. Various adsorbents (*e.g.*, carbon nanotubes and clays)[5–14] have been extensively utilized for carbon dioxide capture. In enhanced oil recovery (EOR) operations, the oil recovery could also be combined with the carbon dioxide storage.[15–21] The water-alternating-gas (WAG) approach has been utilized for mobility control during CO_2-EOR operations.[16,18,19,21] The WAG cycles consist of injecting water (or surfactant) and CO_2 alternately into the reservoirs. Lowering the interfacial tension (IFT) of the oil + water system leads to an increase in the capillary number,[17,20] which may help to recover more oil. In general, the presence of surfactant/CO_2 decreased this IFT. In addition, the captured CO_2 contains impurities (*e.g.*, CH_4)[7,22–24] that may have an important influence on the EOR operations.

Physical Science and Engineering Division (PSE), Computational Transport Phenomena Laboratory, King Abdullah University of Science and Technology (KAUST), Thuwal, 23955-6900, Saudi Arabia.

E-mail: arun.narayanannair@kaust.edu.sa, shuyu.sun@kaust.edu.sa

† Electronic supplementary information (ESI) available: Additional details of simulation analysis. See DOI: 10.1039/d1sm01267c

Experiments,[25–37] theory,[32–34,36–39] and simulations[38–45] have been successfully employed to understand the bulk and interfacial properties of alkane + water + CH_4/CO_2 systems. These studies have reported the occurrence of, for example, a two-phase region at high pressures. The IFT of the alkane + water + CH_4/CO_2 two-phase systems was more similar to that of the corresponding alkane + water system alone.[25,35,36,38–43,45] The IFTs of the alkane + water + CH_4/CO_2 and alkane + brine + CH_4/CO_2 systems increased with decreasing x_{CH_4}/x_{CO_2} (x_{CH_4} and x_{CO_2} are the mole fractions of CH_4 and CO_2 in the alkane-rich phase, respectively). This can be attributed to the fact that the interface was enriched with CH_4 and CO_2 molecules.[38–43] The IFTs of the alkane + brine and alkane + brine + CH_4/CO_2 systems were reported to increase with increasing salt concentration.[26,27,29,39,44,45] It is also known that the addition of surfactants such as sodium dodecyl sulfate (SDS) generally decreases the IFT.[46–58] Molecular simulations showed that, in the water + surfactant system, water molecules and sodium counterions are relatively near the SDS headgroups.[49,51–58] Bruce *et al.* found distortions in the water–water hydrogen bonding network because of the SDS–water hydrogen bond formations.[49] Lin *et al.* found that, in the water + surfactant + CH_4 system, the solubility of CH_4 in water is not affected by the presence of SDS molecules at the interface.[55] da Rocha *et al.*

observed favorable CO_2-fluorinated surfactant tail interactions at the interface in the water + surfactant + CO_2 system.[50] The high density of CO_2 in the bulk enabled strong interaction between CO_2 and the hydrocarbon tail of SDS at the interface.[56,57] However, the interfacial behavior of the decane + brine + surfactant + CH_4 + CO_2 system has not been studied yet.

Molecular simulations have emerged as important tools for accurately predicting the bulk and interfacial properties.[9,12–14,38,59–62] Here, we perform molecular dynamics (MD) simulations to get insights into the interfacial behavior of the decane + brine + surfactant system in the presence of CH_4 and CO_2 at reservoir conditions.

2 Simulation details

MD simulations of decane + water + surfactant and decane + brine + surfactant two-phase systems in the presence of CH_4 and CO_2 at 323 and 443 K, and pressure up to 100 MPa were carried out using the GROMACS package.[63] The salt (NaCl) concentration is 2.7 mol kg^{-1} and the amounts of surfactant adsorbed at the interface are 0.008 and 0.016 SDS per Å^2. The method is similar to that used previously by us.[39,64,65] In short, the TraPPE force field was used to model normal decane, methane, and carbon dioxide.[66–68] Water is represented by the TIP4P/2005 model[69] and the Na$^+$ and Cl$^-$ ions are described using the Smith and Dang[70] parameters. As in the case of, e.g., decane, the hydrocarbon tail of SDS (C12) was also modeled using the TraPPE united atom force field. The sulfate head group of SDS was modeled using the all-atom CHARMM36 forcefield.[71] The Lennard-Jones energy (ε) and distance (σ) parameters, and the charges (q) of the SDS molecules are given in Table 1. The number of each species employed in our simulations is given in Table 2. For example, all the systems had 2048 water and 200 decane molecules. Also, all the systems had the dimensions of 36 × 36 Å parallel to the interfaces (Fig. 1). The cell size in the z-direction (perpendicular to the interfaces) L_z was about three times this value. The system sizes used here ensure that the finite-size effects are negligible.[38,40–43,72–74] Each system was equilibrated for 5 ns in the NPT ensemble (only L_z varied) and we ran a 5 ns production under NVE conditions. The temperature was controlled using the Nosé–Hoover thermostat and pressure using the Parrinello–Rahman barostat.

The IFT was estimated from the below equation:[38,39,64,65,72–75]

$$\gamma = \frac{1}{2}L_z\left[P_{zz} - \frac{1}{2}(P_{xx} + P_{yy})\right], \qquad (1)$$

Table 1 Force field parameters of SDS

Site	σ (Å)	ε (kJ mol^{-1})	q (e)	Ref.
O	3.029	0.502	−0.650	71
S	3.741	1.966	1.330	71
O (in O–C bond)	2.939	0.418	−0.280	71
CH$_2$ (in O–C bond)	3.950	0.382	−0.100	66
CH$_2$	3.950	0.382	0	66
CH$_3$	3.750	0.815	0	66

where the diagonal components of the pressure tensor are represented by P_{xx}, P_{yy}, and P_{zz}. The radial distribution function (RDF) was determined as described previously.[14] The validation of models and a detailed analysis of the interfacial behavior of decane + H_2O and decane + brine (NaCl) systems in the presence of CH_4, CO_2, and their mixture can be found in our previous studies.[38,39] The amounts of surfactant chosen in our simulations (0.008 and 0.016 SDS per Å^2) seem to be well below the critical micelle concentration (CMC). The overlap of the simulated IFTs of the water + SDS and water + SDS + CH_4 systems with the corresponding experimental data[46,47] is shown in Fig. 2. To achieve the overlap, the bulk concentration of surfactant reported in the experiments was multiplied by a constant (same value used in both systems). It is important to mention that these estimates could be further improved by using the Gibbs adsorption isotherm.[55,58] For these systems, the CMC is about 8 mM (about 0.025 SDS per Å^2 [76,77]). Note, however, that higher surfactant concentrations might be considered by using coarse-grained models.[78]

3 Results

3.1 Interfacial tension

The simulated IFTs of the decane + water + surfactant and decane + brine + surfactant systems in the presence of CH_4 (x_{CH_4} = 0.5), CO_2 (x_{CO_2} = 0.5), and their equimolar mixture (x_{CH_4} = x_{CO_2} = 0.25) at 443 K are provided in Fig. 3. The salt (NaCl) concentration was 2.7 mol kg^{-1} and the amounts of surfactant adsorbed at the interface were 0.008 and 0.016 SDS per Å^2. The corresponding simulation results at 323 K are provided in Fig. S1 (ESI†). Note that our previous results of the simulated IFTs of the decane + water[38] and decane + brine (NaCl)[39] systems in the presence of CH_4, CO_2, and their mixture compared well with the corresponding experimental[25,35] and density gradient theory (DGT)[38,39] results. Past studies have shown that the IFT of the alkane + water + CH_4/CO_2 systems is more similar to that of the corresponding alkane + water system alone.[25,35,36,38–43,45] Also, the IFT of the decane + brine + CH_4/CO_2 systems was more similar to that of the corresponding decane + brine system alone.[26,29,39,44,45] The IFTs of all these systems decreased with temperature. For instance, the simulation value of the IFT of the decane + water system (20 MPa) decreased from about 47.8 mN m^{-1} at 323 K to about 36.5 mN m^{-1} at 443 K.[39] It was found that the IFTs of these systems generally increased with pressure. The influence of pressure was, however, found to be less pronounced at lower temperatures and higher values of x_{CH_4}/x_{CO_2}. Note that the IFT of the water + CH_4/CO_2 and brine + CH_4/CO_2 systems depends nonmonotonically on pressure.[72–75,79–88] Furthermore, the IFTs of the alkane + water + CH_4/CO_2 and alkane + brine + CH_4/CO_2 systems increased with decreasing x_{CH_4}/x_{CO_2}. Here, the influence of methane was found to be less pronounced than that of carbon dioxide. This can be attributed to the fact that the interface was highly enriched with CO_2 molecules than with methane molecules. It was found that the IFTs of the alkane + brine and

Table 2 Number of molecules used in MD simulations

| System	Water no.	Decane no.	CH_4 no.	CO_2 no.	Na^+/Cl^- no.	SDS no.
Water + decane + SDS	2048	200				20–40
Brine + decane + SDS	2048	200			100	20–40
Water + 50%decane + 50%CH_4 + SDS	2048	200	200			20–40
Brine + 50%decane + 50%CH_4 + SDS	2048	200	200		100	20–40
Water + 50%decane + 50%CO_2 + SDS	2048	200		200		20–40
Brine + 50%decane + 50%CO_2 + SDS	2048	200		200	100	20–40
Water + 50%decane + 25%CH_4 + 25%CO_2 + SDS	2048	200	100	100		20–40
Brine + 50%decane + 25%CH_4 + 25%CO_2 + SDS	2048	200	100	100	100	20–40
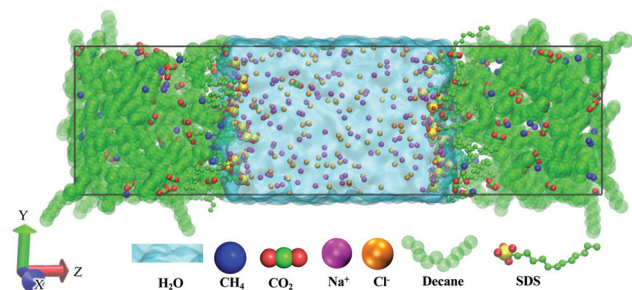
Fig. 1 Equilibrium snapshot of the decane + brine + surfactant + CH_4 + CO_2 ($x_{CH_4} = x_{CO_2} = 0.25$) system at 443 K and 20 MPa. The NaCl concentration is 2.7 mol kg^{-1} and the amount of surfactant adsorbed at the interface is 0.016 SDS per Å^2.

alkane + brine + CH_4/CO_2 systems increase with salt concentration.[26,27,29,39,44,45] Here, the linear slope in the IFT *versus* salt (NaCl) concentration plot was about 2 mN (m mol kg^{-1})$^{-1}$ under all conditions. This value was similar to that reported for the brine + CH_4/CO_2 systems.[72,73,79] However, higher slopes were reported for the corresponding systems containing divalent ions.[73,79]

Previous studies[47,55] have also shown that the IFTs decreased with increasing SDS concentration, *e.g.*, at the methane/water interface (see Fig. 2). Our current results show that the addition of the SDS surfactant reduces the IFTs of the decane + water and decane + water + CH_4/CO_2 systems. Similar behavior is also observed for the decane + brine and decane + brine + CH_4/CO_2

systems. For example, the IFT of the decane + water + surfactant (0.016 SDS per Å^2) system is about 16.5 mN m^{-1} at 20 MPa and 443 K. As in the case of, for example, the alkane + water system, the IFTs of these surfactant containing systems decrease with temperature and the influence of pressure is found to be less pronounced. We see that the IFTs of the decane + water + surfactant + CH_4/CO_2 and decane + brine + surfactant + CH_4/CO_2 systems decrease with increasing x_{CH_4}/x_{CO_2}. Again the influence of methane is found to be less pronounced than that of carbon dioxide. For example, the IFTs of the decane + water + surfactant (0.016 SDS per Å^2) system in the presence of CH_4 ($x_{CH_4} = 0.5$) and CO_2 ($x_{CO_2} = 0.5$) were about 13.7 and 11.5 mN m^{-1}, respectively, at 20 MPa and 443 K. It can be seen that the IFT of, for instance, the decane + water + surfactant + CH_4 + CO_2 system is more similar to that of the corresponding decane + water + surfactant + CO_2 system. Furthermore, the addition of salt increased the IFTs of the decane + water + surfactant and decane + water + surfactant + CH_4/CO_2 systems. For example, the IFT of the decane + brine + surfactant (0.016 SDS per Å^2) system is about 25.2 mN m^{-1} at 20 MPa and 443 K.

3.2 Atomic density profiles

The atomic density profiles may provide insights into the bulk and interfacial properties of the studied systems. The simulated density profiles for the decane + brine + surfactant + CH_4 + CO_2 ($x_{CH_4} = x_{CO_2} = 0.25$) system at 443 K and 20 MPa are provided in Fig. 4. These profiles at other conditions are provided in Fig. S2–S4 (ESI†). Note that our simulation results of the atomic density
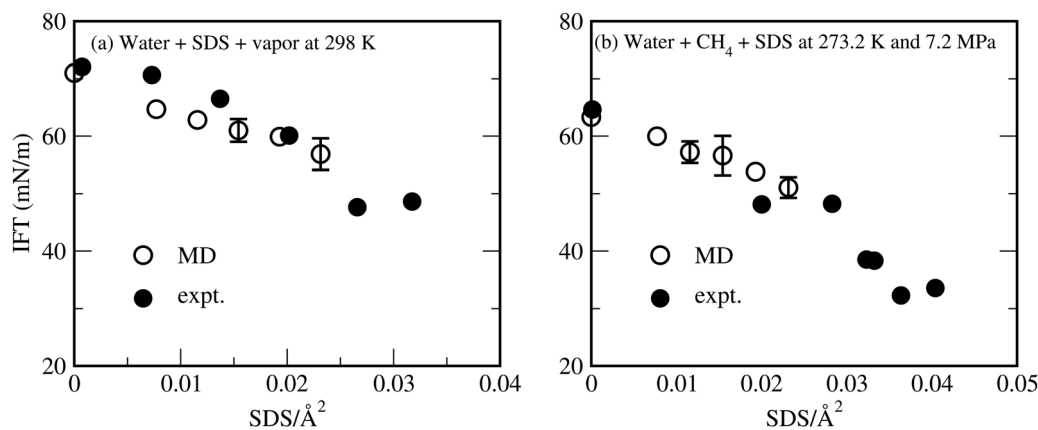

Fig. 2 IFT dependence on the surface concentration of surfactant for the (a) water + surfactant system at 298 K and (b) water + surfactant + CH_4 system at 273.2 K and 7.2 MPa.
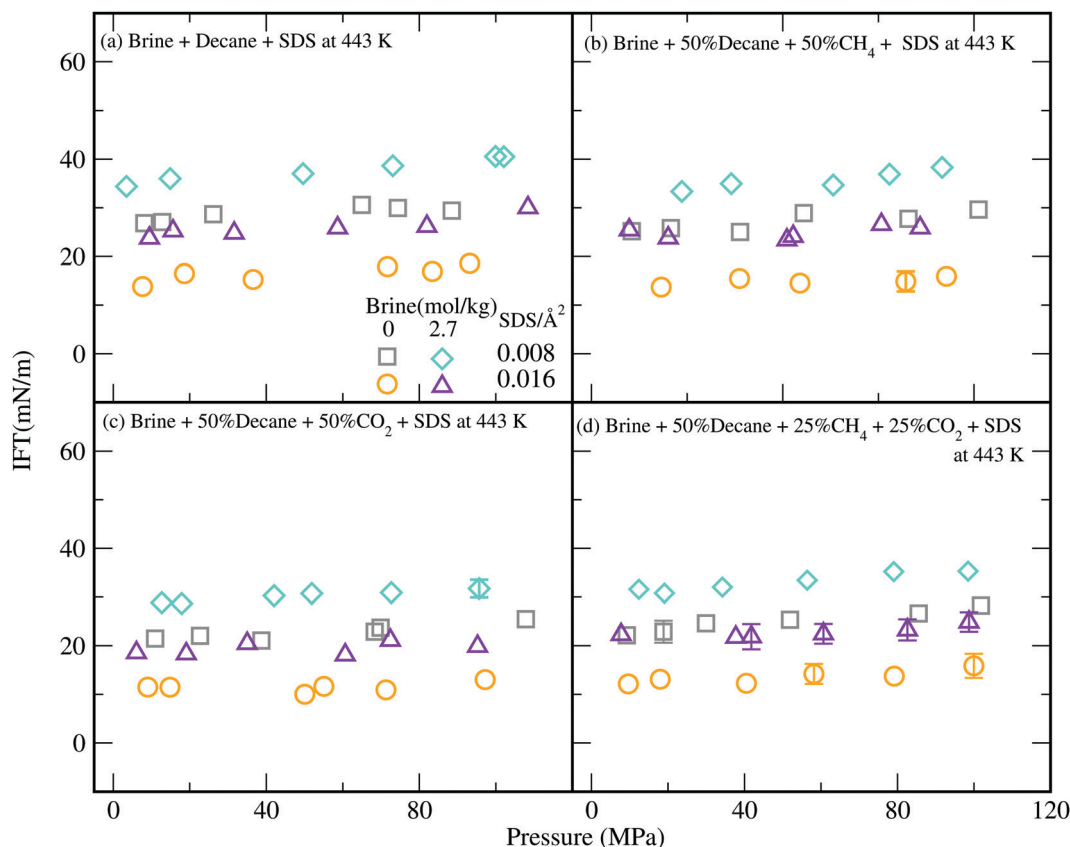
Fig. 3 IFTs of (a) decane + brine + surfactant, (b) decane + brine + surfactant + CH_4 (x_{CH_4} = 0.5), (c) decane + brine + surfactant + CO_2 (x_{CO_2} = 0.5), and (d) decane + brine + surfactant + CH_4 + CO_2 (x_{CH_4} = x_{CO_2} = 0.25) systems at 443 K. Error bars are smaller than the symbol size.

profiles for the decane + water[38] and decane + brine (NaCl)[39] systems in the presence of CH_4, CO_2, and their mixture compared well with the corresponding DGT[38,39] results. Previous studies of the alkane + water + CH_4/CO_2 and alkane + brine + CH_4/CO_2 systems[36,38–43,45] have shown that the presence of CH_4 and CO_2 hardly affects the density profiles of water, alkane, and salt. It was

found that, in general, the density profiles of water and alkane vary monotonically across the interfacial region. These profiles might be approximated by a hyperbolic tangent function.[89] The salt ions were excluded from the interfacial region and distributed homogenously within the H_2O-rich phase. However, water is enriched at the interfacial region with the addition of salt.[39,73,86,90] This can be
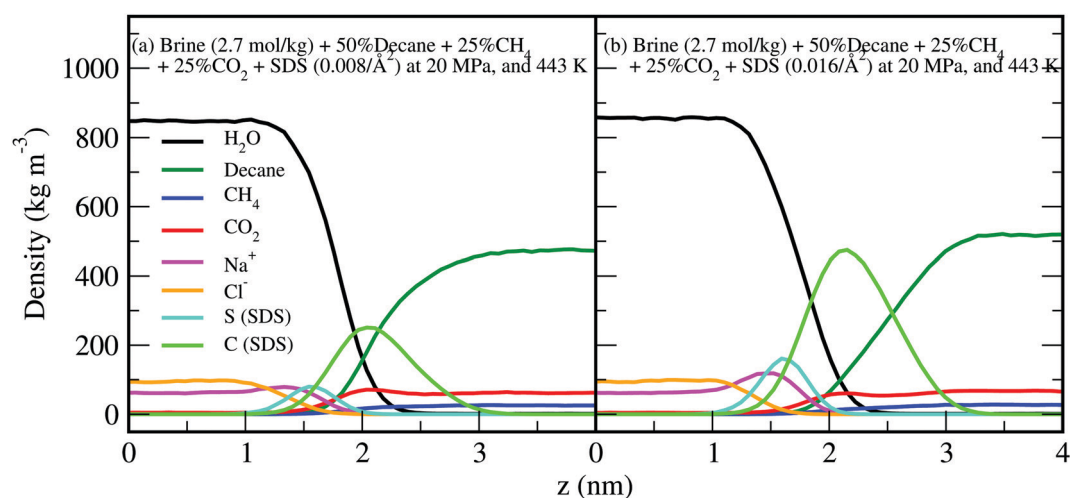

Fig. 4 Atomic density profiles for the decane + brine + surfactant + CH_4 + CO_2 (x_{CH_4} = x_{CO_2} = 0.25) system at 443 K and 20 MPa: (a) 0.008 SDS per Å² and (b) 0.016 SDS per Å². The NaCl concentration is 2.7 mol kg^{-1}.

explained by the enhanced ionic desorption from the interfacial region at high salt concentrations. Also, at high x_{CH_4}, the interfacial region was enriched with decane in the alkane + water + CH_4 system.[38] It is worth noting that the simulated distributions of alkane exhibited artificial oscillations in the interfacial region due to finite-size effects.[89,91] The interfacial region was enriched with CH_4 and CO_2 molecules for the alkane + water + CH_4/CO_2 and alkane + brine + CH_4/CO_2 systems.[36,38–43,45] This enrichment was found to decrease with temperature and increase with pressure. Also, in general, this enrichment increased with increasing x_{CH_4}/x_{CO_2}. Here, the enrichment of methane was found to be less pronounced than that of carbon dioxide. The presence of salt had no significant effect on the CH_4/CO_2 enrichment.[39] At low pressures, however, the enrichment of the interfacial region with CO_2 (CH_4) depends nonmonotonically on x_{CO_2} (x_{CH_4}).[38,40] Details of the interfacial behavior of the water + CH_4/CO_2 and brine + CH_4/CO_2 systems have been described by us and others.[72–75,80–84,86–88] Here the enrichment of the interfacial region with CH_4 and CO_2 depends nonmonotonically on pressure.

Note that the behavior of the IFT can be further understood by means of the Gibbs adsorption equation:

$$-d\gamma = \sum_i \Gamma_i d\mu_i, \quad (2)$$

where Γ_i and μ_i are the surface excess and the chemical potential of component i, respectively. The surface excesses could be calculated using the density profiles.[38,39,64,65,73,74,84,85] A detailed description of the surface excess of different species in the decane + water + CH_4/CO_2 and decane + brine + CH_4/CO_2 systems is provided in our previous reports.[38,39] For these systems, it was found that the IFTs increase with pressure (salt concentration) due to the negative surface excesses of alkanes (salt).[38,39] For the water + CH_4/CO_2 and brine + CH_4/CO_2 systems, a minimum was found in the IFT *versus* pressure plot when the surface excess of CH_4/CO_2 changes sign from positive to negative.[73,75,84,85] Furthermore, for the alkane + water and alkane + water + CH_4/CO_2 systems, the solubilities of decane/CH_4/CO_2 in the water-rich phase and water in the decane-rich phase were very low.[38,92,93] The solubility of CH_4/CO_2 in the water-rich phase was found to decrease with the addition of salt (salting-out effect).[39]

Our current results show that the sulfate head groups (see, *e.g.*, sulfur atoms) of the SDS surfactant molecules penetrate the water-rich phase and their alkyl tails are stretched into the decane-rich phase. The Na$^+$ counterions of the SDS surfactant molecules are located very close to their head groups (see, *e.g.*, Fig. S2, ESI†). Furthermore, the distributions of water and Cl$^-$ ions are independent of the surfactant concentration for the
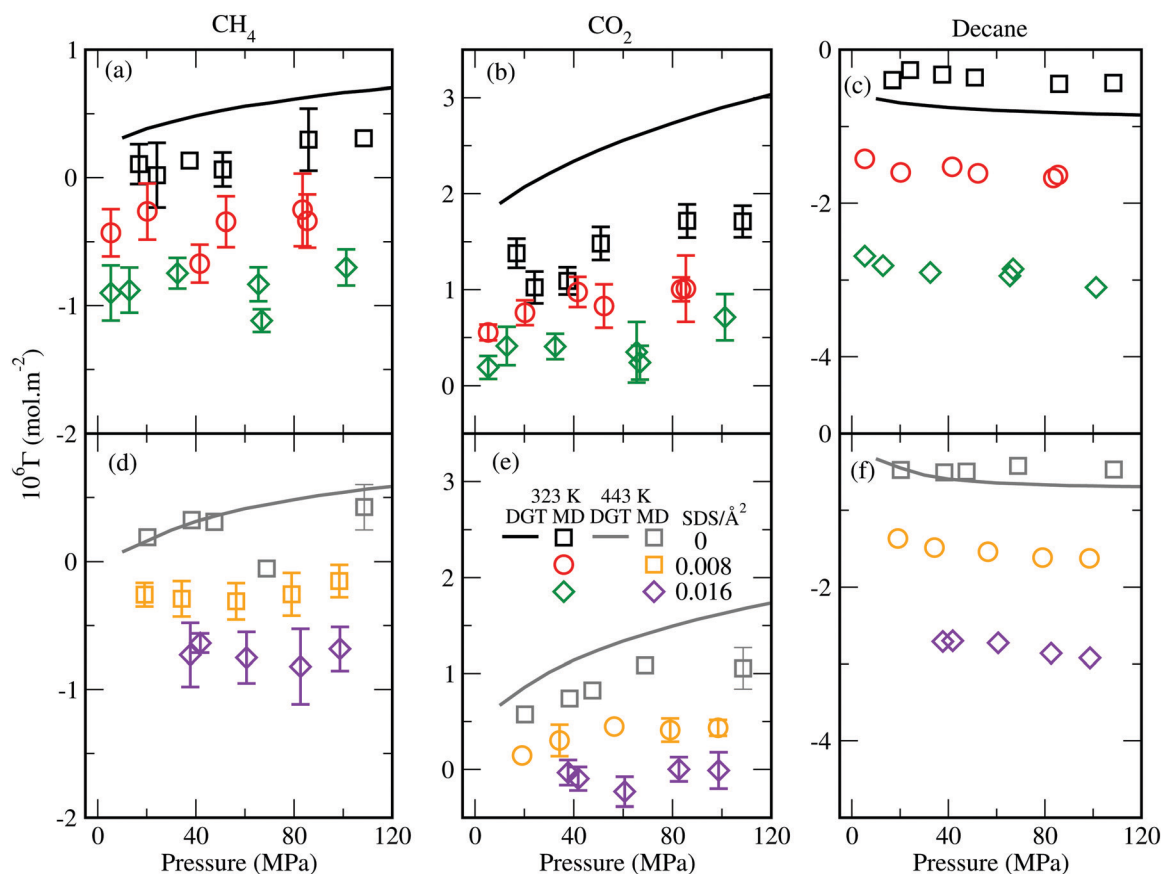

Fig. 5 Simulated surface excess (symbols) of (a) CH_4, (b) CO_2, and (c) decane for the decane + brine + surfactant + CH_4 + CO_2 ($x_{CH_4} = x_{CO_2} = 0.25$) system at 323 K and NaCl concentration of 2.7 mol kg^{-1}. The corresponding surface excess at 443 K is shown in (d), (e), and (f), respectively. The lines denote the DGT results.[39]

studied systems (see also Fig. S5, ESI†). However, the interfacial thickness between water and decane/CH_4/CO_2 molecules increases with increasing surfactant concentration. We estimated the interfacial thickness between water and decane by applying the "90–90" interfacial thickness criterion (distance between positions where densities of decane and H_2O were 90% of their own bulk densities).[51] The results are provided in Fig. S6–S9 (ESI†). The interfacial thickness between water and decane is in the range of about 1.1–1.7 nm for the studied systems. This interfacial thickness shows an opposite trend to that seen for the IFT. For example, the interfacial thickness decreases with the addition of salt and increases with the addition of CH_4/CO_2. Interestingly, the enrichment of CH_4 and/or CO_2 in the interfacial region decreases with increasing surfactant concentration. It seems that the enrichment is followed by a minimum in the density profile of CO_2 at high surfactant concentrations. This minimum is found near the location of the surfactant tails.

We calculated the surface excess[38,39,64,65,73,74,84,85] by using these density profiles. Our results show that the surface excess of CH_4, CO_2, and decane decreases with increasing surfactant concentration (Fig. 5). The surface excess of CH_4/CO_2 changes sign from positive to negative as surfactant concentration increases. The addition of SDS surfactants has a more pronounced effect on the surface excess of decane. For example, at 443K and 20 MPa, the surface excess of decane in the decane + brine + CH_4 + CO_2[39] and decane + brine + surfactant + CH_4 + CO_2 (0.016 SDS per Å^2) systems is about -0.47×10^{-6} mol m^{-2} and -2.7×10^{-6} mol m^{-2}, respectively. The corresponding surface excess of CH_4 is about 0.19×10^{-6} mol m^{-2} and -0.73×10^{-6} mol m^{-2}, respectively, and that of CO_2 is about 0.57×10^{-6} mol m^{-2} and -0.03×10^{-6} mol m^{-2}, respectively. Here the effects of pressure, temperature, and mole fraction on the surface excess are similar to those observed for the decane + water + CH_4/CO_2 and decane + brine + CH_4/CO_2 systems.[38,39] For example in all cases, we see that the surface excess of decane decreases with pressure, whereas the surface excess of CH_4 and CO_2 increases with pressure.

3.3 Radial distribution functions

The RDFs may give further insights into the interfacial properties of the surfactant-containing systems. The simulated RDFs for the decane + brine + surfactant + CH_4 + CO_2 system at 443 K and 20 MPa are provided in Fig. 6. We see that water molecules and counterions are nearest to the SDS headgroups. The first peak in the RDF of S–H (water), S–Na$^+$, and S–O (water) is around 0.29, 0.36, and 0.38 nm, respectively. These peak positions obtained here are consistent with the previous simulation results.[52–54,58] The presence of water molecules near the SDS headgroups is possibly due to the hydrogen bonding between SDS headgroups and water molecules.[49] Whereas, CO_2, CH_4, decane, and Cl$^-$ are further away from the SDS headgroups. The first peak in the RDF of S–O (CO_2), S–CH_4 site, and S–Cl$^-$ is around 0.40, 0.46, and 0.49 nm, respectively. The RDFs show that the interactions of the surfactant headgroups with methane are weaker than those with CO_2. This is expected due to the quadrupole moment of CO_2 molecule.[94] Similar positions of these peaks were found in all studied systems. It is worth mentioning that here the RDFs may
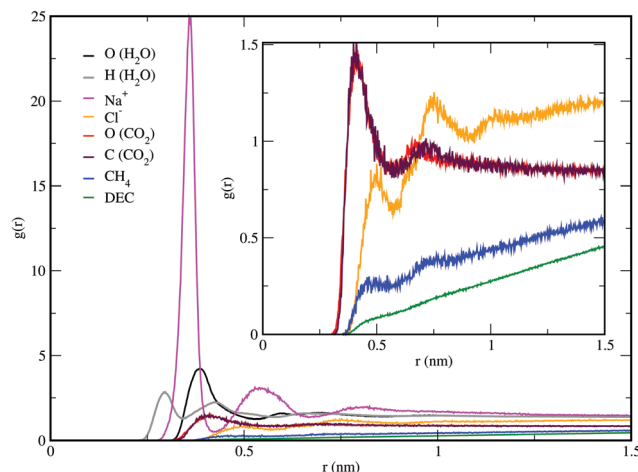

Fig. 6 RDFs between the S-atom of SDS and different species in the decane + brine + surfactant + CH_4 + CO_2 (x_{CH_4} = x_{CO_2} = 0.25) system at 443 K and 20 MPa. The NaCl concentration is 2.7 mol kg^{-1} and the amount of surfactant adsorbed at the interface is 0.016 SDS per Å^2.

not go to unity at large distances due to the inhomogeneous nature of the system.[52–54,58] In comparison, the alkyl tails of SDS interact strongly with decane molecules leading to peaks, for example, at 0.55 nm (Fig. S10, ESI†). Furthermore, it is found that the alkyl tails of SDS interact similarly with CH_4 and CO_2. For both these interactions the first peak in the RDF plot is around 0.47 nm and its magnitude is about 1.7. A similar result is obtained for the interactions between alkane and CH_4/CO_2.[64,65]

We calculated the end-to-end distance and radius of gyration[62,64,65] of the alkyl tails of SDS molecules for the decane + water + surfactant system (Table 3). Here the end-to-end distance is in the range of about 1.12 to 1.18 nm. This end-to-end distance decreases with temperature and increases with the amount of surfactant. We found that pressure has no effect on the end-to-end distance. Similar trends were observed for the radius of gyration. Furthermore, these sizes were not affected by the presence of salt/CH_4/CO_2 under the studied conditions.

Regarding the SDS force field (see Table 1), it was shown that the difference among the force fields does not have much effect on the overall structure of small aggregates of surfactant.[54] Among different water models, the surface tension simulated using TIP4P/2005 model was close to the experimental data.[72] Moreover, our simulated RDF peaks for SDS–water spatial correlations are consistent with previous studies.[52–54,58] It will be challenging to obtain the relevant activity coefficients of, e.g., salt from molecular simulations for these multi-component

Table 3 Chain size of the alkyl tail (C12) of SDS for the decane + water + surfactant system at 20 MPa

No. of SDS per Å^2	End to end distance/radius of gyration (nm)	
	323 K	443 K
0.008	1.16/0.394	1.12/0.383
0.016	1.18/0.396	1.14/0.385

systems.[95] However, for decane + brine + CH_4/CO_2 systems, theoretical analysis showed that changing salt concentration does not have much effect on the chemical potential of decane, CH_4, and CO_2.[38,39] This explains the fact that the IFTs increased with salt concentration because of the negative surface excess of salt ions (see eqn (2)).[38,39] Note that we did not consider any SDS in the bulk and the salting-out of SDS to the interface.[48] Therefore, further studies are necessary to fully understand the effects of surfactants on the decane + brine + CH_4/CO_2 systems.

4 Conclusions

The interfacial behavior of the decane + brine + surfactant + $CH_4 + CO_2$ two-phase system was studied using MD simulations at 323 and 443 K, and pressure up to 100 MPa. Note that our previous results[38,39] of the simulated IFTs of decane + brine + CH_4/CO_2 systems compared well with the corresponding experimental[25,35] and DGT[38,39] results. Our current results show that the addition of CH_4, CO_2, and the presence of SDS surfactant at the interface reduced the IFTs of the decane + water and decane + brine (NaCl) systems. Notably, the influence of methane was observed to be less pronounced than that of carbon dioxide. For example, the IFT of the decane + water + SDS + $CH_4 + CO_2$ ($x_{CH_4} = x_{CO_2} = 0.25$) system is more similar to that of the corresponding decane + water + SDS + CO_2 ($x_{CO_2} = 0.5$) system. This may be attributed to the fact that the interface was highly enriched with CO_2 molecules than with CH_4 molecules. As expected, at a fixed surface concentration of SDS, the addition of salt increases the IFTs of the decane + water + SDS and decane + water + SDS + CH_4/CO_2 systems. The IFTs of these surfactant-containing systems decreased with temperature and the influence of pressure was found to be less pronounced.

The atomic density profiles show that the sulfate head groups of the SDS molecules penetrate the water-rich phase and their alkyl tails are stretched into the decane-rich phase. The Na^+ counterions of the surfactant molecules are positioned very close to their head groups. Furthermore, the density profiles of water and salt ions are independent of the surfactant concentration. However, the interfacial thickness between water and decane/CH_4/CO_2 molecules increases with increasing surfactant concentration. For instance, the interfacial thickness between water and decane is in the range of about 1.1–1.7 nm for the studied systems. This interfacial thickness decreased with the addition of salt and increased with the addition of CH_4/CO_2. An important finding is that the enrichment of CH_4 and/or CO_2 in the interfacial region decreases with increasing surfactant concentration. The calculated RDFs show that the interactions of the surfactant headgroups with methane are weaker than those with CO_2.

Conflicts of interest

There are no conflicts to declare.

Acknowledgements

References

1 E. Houghton, *Climate change 1995: The science of climate change: contribution of working group I to the second assessment report of the Intergovernmental Panel on Climate Change*, Cambridge University Press, 1996, vol. 2.

2 P. M. Cox, R. A. Betts, C. D. Jones, S. A. Spall and I. J. Totterdell, Acceleration of global warming due to carbon-cycle feedbacks in a coupled climate model, *Nature*, 2000, **408**, 184.

3 F. Birol, *CO₂ Emissions From Fuel Combustion Highlights, 2016.*

4 C. J. Rhodes, The 2015 Paris climate change conference: COP21, *Sci. Progr.*, 2016, **99**, 97–104.

5 S. Kim, J. R. Jinschek, H. Chen, D. S. Sholl and E. Marand, Scalable fabrication of carbon nanotube/polymer nanocomposite membranes for high flux gas transport, *Nano Lett.*, 2007, **7**, 2806–2811.

6 H. Yang, Z. Xu, M. Fan, R. Gupta, R. B. Slimane, A. E. Bland and I. Wright, Progress in carbon dioxide separation and capture: A review, *J. Environ. Sci.*, 2008, **20**, 14–27.

7 D. M. D'Alessandro, B. Smit and J. R. Long, Carbon dioxide capture: Prospects for new materials, *Angew. Chem., Int. Ed.*, 2010, **49**, 6058–6082.

8 N. Rangnekar, N. Mittal, B. Elyassi, J. Caro and M. Tsapatsis, Zeolite membranes – A review and comparison with MOFs, *Chem. Soc. Rev.*, 2015, **44**, 7128–7154.

9 A. Kadoura, A. K. Narayanan Nair and S. Sun, Molecular simulation study of montmorillonite in contact with variably wet supercritical carbon dioxide, *J. Phys. Chem. C*, 2017, **121**, 6199–6208.

10 G. Kupgan, L. J. Abbott, K. E. Hart and C. M. Colina, Modeling amorphous microporous polymers for CO_2 capture and separations, *Chem. Rev.*, 2018, **118**, 5488–5538.

11 V. Romanov, *Greenhouse Gases and Clay Minerals: Enlightening Down-to-Earth Road Map to Basic Science of Clay-Greenhouse Gas Interfaces*, Springer, 2018.

12 Y. Yang, A. K. Narayanan Nair and S. Sun, Adsorption and diffusion of methane and carbon dioxide in amorphous regions of cross-linked polyethylene: A molecular simulation study, *Ind. Eng. Chem. Res.*, 2019, **58**, 8426–8436.

13 Y. Yang, A. K. Narayanan Nair and S. Sun, Adsorption and diffusion of carbon dioxide, methane, and their mixture in carbon nanotubes in the presence of water, *J. Phys. Chem. C*, 2020, **124**, 16478–16487.

14 Y. Yang, A. K. Narayanan Nair and S. Sun, Sorption and diffusion of methane and carbon dioxide in amorphous poly(alkyl acrylates): A molecular simulation study, *J. Phys. Chem. B*, 2020, **124**, 1301–1310.

15 M. LangstonS. HoadleyD. Young*et al.*, Definitive CO_2 flooding response in the SACROC unit, in *SPE Enhanced Oil Recovery Symposium*, 1988.

16 R. Farajzadeh, A. Andrianov and P. Zitha, Investigation of immiscible and miscible foam for enhancing oil recovery, *Ind. Eng. Chem. Res.*, 2010, **49**, 1910–1919.

17 C. Zhang, M. Oostrom, T. W. Wietsma, J. W. Grate and M. G. Warner, Influence of viscous and capillary forces on immiscible fluid displacement: Pore-scale experimental study in a water-wet micromodel demonstrating viscous and capillary fingering, *Energy Fuels*, 2011, **25**, 3493–3505.

18 R. M. Enick and D. K. Olsen, Mobility and conformance control for carbon dioxide enhanced oil recovery (CO$_2$-EOR) *via* thickeners, foams, and gels – A detailed literature review of 40 years of research. Contract DE-FE0004003, *Activity*, 2012, **4003**, 01.

19 Z. Dai, H. Viswanathan, R. Middleton, F. Pan, W. Ampomah, C. Yang, W. Jia, T. Xiao, S.-Y. Lee and B. McPherson, *et al.*, CO$_2$ accounting and risk analysis for CO$_2$ sequestration at enhanced oil recovery sites, *Environ. Sci. Technol.*, 2016, **50**, 7546–7554.

20 H. Zhang, T. Ramakrishnan, A. Nikolov and D. Wasan, Enhanced oil recovery driven by nanofilm structural disjoining pressure: Flooding experiments and microvisualization, *Energy Fuels*, 2016, **30**, 2771–2779.

21 G. Jian, L. Zhang, C. Da, M. Puerto, K. P. Johnston, S. L. Biswal and G. J. Hirasaki, Evaluating the transport behavior of CO$_2$ foam in the presence of crude oil under high-temperature and high-salinity conditions for carbonate reservoirs, *Energy Fuels*, 2019, **33**, 6038–6047.

22 A. A. Olajire, CO$_2$ capture and separation technologies for end-of-pipe applications – A review, *Energy*, 2010, **35**, 2610–2628.

23 H. Li, J. P. Jakobsen, Ø. Wilhelmsen and J. Yan, PVTxy properties of CO$_2$ mixtures relevant for CO$_2$ capture, transport and storage: Review of available experimental data and theoretical models, *Appl. Energy*, 2011, **88**, 3567–3579.

24 S. T. Blanco, C. Rivas, J. Fernandez, M. Artal and I. Velasco, Influence of methane in CO$_2$ transport and storage for CCS technology, *Environ. Sci. Technol.*, 2012, **46**, 13016–13023.

25 H. Y. Jennings and G. H. Newman, The effect of temperature and pressure on the interfacial tension of water against methane-normal decane mixtures, *Soc. Petrol. Eng. J.*, 1971, **11**, 171–175.

26 R. Aveyard and S. M. Saleem, Interfacial tensions at alkane–aqueous electrolyte interfaces, *J. Chem. Soc., Faraday Trans. 1*, 1976, 1609–1617.

27 N. Ikeda, M. Aratono and K. Motomura, Thermodynamic study on the adsorption of sodium chloride at the water/hexane interface, *J. Colloid Interface Sci.*, 1992, **149**, 208–215.

28 G. Brunner, J. Teich and R. Dohrn, Phase equilibria in systems containing hydrogen, carbon dioxide, water and hydrocarbons, *Fluid Phase Equilib.*, 1994, **100**, 253–268.

29 B.-Y. Cai, J.-T. Yang and T.-M. Guo, Interfacial tension of hydrocarbon + water/brine systems under high pressure, *J. Chem. Eng. Data*, 1996, **41**, 493–496.

30 C.-Y. Sun and G.-J. Chen, Measurement of interfacial tension for the CO$_2$ injected crude oil+ reservoir water system, *J. Chem. Eng. Data*, 2005, **50**, 936–938.

31 D. Yang, P. Tontiwachwuthikul and Y. Gu, Interfacial tensions of the crude oil + reservoir brine + CO$_2$ systems at pressures up to 31 MPa and temperatures of 27 °C and 58 °C, *J. Chem. Eng. Data*, 2005, **50**, 1242–1249.

32 L. Gil, S. Avila, P. Garca-Giménez, S. Blanco, C. Berro, S. Otin and I. Velasco, Dew points of binary propane or *n*-butane + carbon dioxide, ternary propane or *n*-butane + carbon dioxide + water, and quaternary propane or *n*-butane + carbon dioxide + water + methanol mixtures: Measurement and modeling, *Ind. Eng. Chem. Res.*, 2006, **45**, 3974–3980.

33 A. Bahramian, A. Danesh, F. Gozalpour, B. Tohidi and A. Todd, Vapour–liquid interfacial tension of water and hydrocarbon mixture at high pressure and high temperature conditions, *Fluid Phase Equilib.*, 2007, **252**, 66–73.

34 E. Forte, A. Galindo and J. M. Trusler, Experimental and molecular modeling study of the three-phase behavior of (*n*-decane + carbon dioxide + water) at reservoir conditions, *J. Phys. Chem. B*, 2011, **115**, 14591–14609.

35 A. Georgiadis, G. Maitland, J. M. Trusler and A. Bismarck, Interfacial tension measurements of the (H2O + *n*-decane + CO$_2$) ternary system at elevated pressures and temperatures, *J. Chem. Eng. Data*, 2011, **56**, 4900–4908.

36 L. M. C. PereiraA. ChapoyB. Tohidi*et al.*, Vapor-liquid and liquid–liquid interfacial tension of water and hydrocarbon systems at representative reservoir conditions: Experimental and modelling results, in *SPE Annual Technical Conference and Exhibition*, 2014.

37 S. Z. Al Ghafri, E. Forte, A. Galindo, G. C. Maitland and J. M. Trusler, Experimental and modeling study of the phase behavior of (heptane + carbon dioxide + water) mixtures, *J. Chem. Eng. Data*, 2015, **60**, 3670–3681.

38 Y. Yang, A. K. Narayanan Nair, M. F. Anwari Che Ruslan and S. Sun, Bulk and interfacial properties of the decane + water system in the presence of methane, carbon dioxide, and their mixture, *J. Phys. Chem. B*, 2020, **124**, 9556–9569.

39 N. Choudhary, M. F. A. Che Ruslan, A. K. Narayanan Nair, R. Qiao and S. Sun, Bulk and interfacial properties of the decane + brine system in the presence of carbon dioxide, methane, and their mixture, *Ind. Eng. Chem. Res.*, 2021, **60**, 11525–11534.

40 L. Zhao, L. Tao and S. Lin, Molecular dynamics characterizations of the supercritical CO$_2$-mediated hexane-brine interface, *Ind. Eng. Chem. Res.*, 2015, **54**, 2489–2496.

41 B. Liu, J. Shi, M. Wang, J. Zhang, B. Sun, Y. Shen and X. Sun, Reduction in interfacial tension of water–oil interface by supercritical CO$_2$ in enhanced oil recovery processes studied with molecular dynamics simulation, *J. Supercrit. Fluids*, 2016, **111**, 171–178.

42 J. Zhang, Z. Dong, Y. Zhang, M. Wang and Y. Yan, Effects of the methane content on the water–oil interface: Insights from the molecular level, *Energy Fuels*, 2017, **31**, 7026–7032.

43 S. Mohammed and G. A. Mansoori, The role of supercritical/dense CO$_2$ gas in altering aqueous/oil interfacial properties: A molecular dynamics study, *Energy Fuels*, 2018, **32**, 2095–2103.

44 T. R. Underwood and H. C. Greenwell, The water–alkane interface at various NaCl salt concentrations: A molecular

dynamics study of the readily available force fields, *Sci. Rep.*, 2018, **8**, 1–11.

45 A. Aminian and B. ZareNezhad, Molecular dynamics simulations study on the shear viscosity, density, and equilibrium interfacial tensions of CO_2 + brines and brines + CO_2 + *n*-decane systems, *J. Phys. Chem. B*, 2021, **125**, 2707–2718.

46 T. Sasaki, M. Hattori, J. Sasaki and K. Nukina, Studies of aqueous sodium dodecyl sulfate solutions by activity measurements, *Bull. Chem. Soc. Jpn.*, 1975, **48**, 1397–1403.

47 C.-Y. Sun, G.-J. Chen and L.-Y. Yang, Interfacial tension of methane+ water with surfactant near the hydrate formation conditions, *J. Chem. Eng. Data*, 2004, **49**, 1023–1025.

48 T. D. Gurkov, D. T. Dimitrova, K. G. Marinova, C. Bilke-Crause, C. Gerber and I. B. Ivanov, Ionic surfactants on fluid interfaces: Determination of the adsorption; role of the salt and the type of the hydrophobic phase, *Colloids Surf., A*, 2005, **261**, 29–38.

49 C. D. Bruce, S. Senapati, M. L. Berkowitz, L. Perera and M. D. Forbes, Molecular dynamics simulations of sodium dodecyl sulfate micelle in water: The behavior of water, *J. Phys. Chem. B*, 2002, **106**, 10902–10907.

50 S. R. da Rocha, K. P. Johnston and P. J. Rossky, Surfactant-modified CO_2-water interface: A molecular view, *J. Phys. Chem. B*, 2002, **106**, 13250–13261.

51 S. S. Jang, S.-T. Lin, P. K. Maiti, M. Blanco, W. A. Goddard, P. Shuler and Y. Tang, Molecular dynamics study of a surfactant-mediated decane–water interface: Effect of molecular architecture of alkyl benzene sulfonate, *J. Phys. Chem. B*, 2004, **108**, 12130–12140.

52 H. Domnguez, Self-aggregation of the SDS surfactant at a solid–liquid interface, *J. Phys. Chem. B*, 2007, **111**, 4054–4059.

53 F. Palazzesi, M. Calvaresi and F. Zerbetto, A molecular dynamics investigation of structure and dynamics of SDS and SDBS micelles, *Soft Matter*, 2011, **7**, 9148–9156.

54 X. Tang, P. H. Koenig and R. G. Larson, molecular dynamics simulations of sodium dodecyl sulfate micelles in water – the effect of the force field, *J. Phys. Chem. B*, 2014, **118**, 3864–3880.

55 Z.-Y. Lin, D. T. Wu and S.-T. Lin, Equilibrium and transport properties of methane at the methane/water interface with the presence of SDS, *J. Phys. Chem. C*, 2018, **122**, 29259–29267.

56 J. G. Parra, H. Domnguez, Y. Aray, P. Iza, X. Zarate and E. Schott, Structural and interfacial properties of the CO_2-in-water foams prepared with sodium dodecyl sulfate (SDS): A molecular dynamics simulation study, *Colloids Surf., A*, 2019, **578**, 123615.

57 C. Fan, J. Jia, B. Peng, Y. Liang, J. Li and S. Liu, Molecular dynamics study on CO_2 foam films with sodium dodecyl sulfate: Effects of surfactant concentration, temperature, and pressure on the interfacial tension, *Energy Fuels*, 2020, **34**, 8562–8574.

58 Y. Nan, W. Li and Z. Jin, Ion valency and concentration effect on the structural and thermodynamic properties of brine–decane interfaces with anionic surfactant (SDS), *J. Phys. Chem. B*, 2021, **125**, 9610–9620.

59 N. A. Kumar and C. Seidel, Polyelectrolyte brushes with added salt, *Macromolecules*, 2005, **38**, 9341–9350.

60 N. A. Kumar and V. Ganesan, *Communication: Self-assembly of semiflexible-flexible block copolymers*, 2012.

61 E. B. Stukalin, L.-H. Cai, N. A. Kumar, L. Leibler and M. Rubinstein, Self-healing of unentangled polymer networks with reversible bonds, *Macromolecules*, 2013, **46**, 7525–7541.

62 A. K. Narayanan Nair, A. Martinez Jimenez and S. Sun, Complexation behavior of polyelectrolytes and polyampholytes, *J. Phys. Chem. B*, 2017, **121**, 7987–7998.

63 M. J. Abraham, T. Murtola, R. Schulz, S. Páll, J. C. Smith, B. Hess and E. Lindahl, GROMACS: High performance molecular simulations through multi-level parallelism from laptops to supercomputers, *SoftwareX*, 2015, **1**, 19–25.

64 N. Choudhary, A. K. N. Nair, M. F. A. C. Ruslan and S. Sun, Bulk and interfacial properties of decane in the presence of carbon dioxide, methane, and their mixture, *Sci. Rep.*, 2019, **9**, 1–10.

65 N. Choudhary, M. F. A. Che Ruslan, A. K. Narayanan Nair and S. Sun, Bulk and interfacial properties of alkanes in the presence of carbon dioxide, methane, and their mixture, *Ind. Eng. Chem. Res.*, 2021, **60**, 729–738.

66 M. G. Martin and J. I. Siepmann, Transferable potentials for phase equilibria. 1. United-atom description of n-alkanes, *J. Phys. Chem. B*, 1998, **102**, 2569–2577.

67 J. J. Potoff and J. I. Siepmann, Vapor–liquid equilibria of mixtures containing alkanes, carbon dioxide, and nitrogen, *AIChE J.*, 2001, **47**, 1676–1682.

68 M. SedghiL. Goual *et al.*, Molecular Dynamics Simulations of Asphaltene Dispersion by Limonene and PVAc Polymer During CO_2 Flooding, in *SPE International Conference and Exhibition on Formation Damage Control*, 2016.

69 J. L. Abascal and C. Vega, A general purpose model for the condensed phases of water: TIP4P/2005, *J. Chem. Phys.*, 2005, **123**, 234505.

70 D. E. Smith and L. X. Dang, Computer simulations of NaCl association in polarizable water, *J. Chem. Phys.*, 1994, **100**, 3757–3766.

71 J. Huang, S. Rauscher, G. Nawrocki, T. Ran, M. Feig, B. L. De Groot, H. Grubmüller and A. D. MacKerell, CHARMM36m: An improved force field for folded and intrinsically disordered proteins, *Nat. Methods*, 2017, **14**, 71–73.

72 Y. Yang, A. K. Narayanan Nair and S. Sun, Molecular dynamics simulation study of carbon dioxide, methane, and their mixture in the presence of brine, *J. Phys. Chem. B*, 2017, **121**, 9688–9698.

73 Y. Yang, M. F. A. Che Ruslan, A. K. Narayanan Nair and S. Sun, Effect of ion valency on the properties of the carbon dioxide–methane–brine system, *J. Phys. Chem. B*, 2019, **123**, 2719–2727.

74 L. C. Nielsen, I. C. Bourg and G. Sposito, Predicting CO_2–water interfacial tension under pressure and temperature conditions of geologic CO_2 storage, *Geochim. Cosmochim. Acta*, 2012, **81**, 28–38.

75 J. M. Garrido, H. Quinteros-Lama, J. M. Miguez, F. J. Blas and M. M. Piñeiro, On the physical insight into the barotropic effect in the interfacial behavior for the H2O + CO$_2$ mixture, *J. Phys. Chem. C*, 2019, **123**, 28123–28130.

76 K. Tajima, M. Muramatsu and T. Sasaki, Radiotracer studies on adsorption of surface active substance at aqueous surface. I. Accurate measurement of adsorption of tritiated sodium dodecylsulfate, *Bull. Chem. Soc. Jpn.*, 1970, **43**, 1991–1998.

77 J. R. Lu, A. Marrocco, T. J. Su, R. K. Thomas and J. Penfold, Adsorption of dodecyl sulfate surfactants with monovalent metal counterions at the air-water interface studied by neutron reflection and surface tension, *J. Colloid Interface Sci.*, 1993, **158**, 303–316.

78 A. Ghoufi, P. Malfreyt and D. J. Tildesley, Computer modelling of the surface tension of the gas–liquid and liquid–liquid interface, *Chem. Soc. Rev.*, 2016, **45**, 1387–1409.

79 L. Zhao, J. Ji, L. Tao and S. Lin, Ionic effects on supercritical CO$_2$–brine interfacial tensions: Molecular dynamics simulations and a universal correlation with ionic strength, temperature, and pressure, *Langmuir*, 2016, **32**, 9188–9196.

80 L. M. Pereira, A. Chapoy, R. Burgass, M. B. Oliveira, J. A. Coutinho and B. Tohidi, Study of the impact of high temperatures and pressures on the equilibrium densities and interfacial tension of the carbon dioxide/water system, *J. Chem. Thermodyn.*, 2016, **93**, 404–415.

81 L. M. Pereira, A. Chapoy, R. Burgass and B. Tohidi, Interfacial tension of CO$_2$+ brine systems: Experiments and predictive modelling, *Adv. Water Resour.*, 2017, **103**, 64–75.

82 C. Chalbaud, M. Robin, J. Lombard, F. Martin, P. Egermann and H. Bertin, Interfacial tension measurements and wettability evaluation for geological CO$_2$ storage, *Adv. Water Resour.*, 2009, **32**, 98–109.

83 X. Li, D. A. Ross, J. M. Trusler, G. C. Maitland and E. S. Boek, Molecular dynamics simulations of CO$_2$ and brine interfacial tension at high temperatures and pressures, *J. Phys. Chem. B*, 2013, **117**, 5647–5652.

84 K. Kashefi, L. M. Pereira, A. Chapoy, R. Burgass and B. Tohidi, Measurement and modelling of interfacial tension in methane/water and methane/brine systems at reservoir conditions, *Fluid Phase Equilib.*, 2016, **409**, 301–311.

85 W. Li and Z. Jin, Molecular dynamics simulations of natural gas-water interfacial tensions over wide range of pressures, *Fuel*, 2019, **236**, 480–492.

86 W. Li and Z. Jin, Effect of ion concentration and multivalence on methane–brine interfacial tension and phenomena from molecular perspectives, *Fuel*, 2019, **254**, 115657.

87 P. Naeiji, T. K. Woo, S. Alavi and R. Ohmura, Molecular dynamics simulations of interfacial properties of the CO$_2$–water and CO$_2$–CH4–water systems, *J. Chem. Phys.*, 2020, **153**, 044701.

88 S. Blazquez, I. Zeron, M. Conde, J. Abascal and C. Vega, Scaled charges at work: Salting out and interfacial tension of methane with electrolyte solutions from computer simulations, *Fluid Phase Equilib.*, 2020, **513**, 112548.

89 C. D. Wick, T.-M. Chang, J. A. Slocum and O. T. Cummings, Computational investigation of the *n*-alkane/water interface with many-body potentials: The effect of chain length and ion distributions, *J. Phys. Chem. C*, 2012, **116**, 783–790.

90 H. Peng and M. Firouzi, Evaluation of interfacial properties of concentrated KCl solutions by molecular dynamics simulation, *Colloids Surf., A*, 2018, **538**, 703–710.

91 O. T. Cummings and C. D. Wick, Computational study on the effect of alkyl chain length on alkane–water interfacial width, *Chem. Phys. Lett.*, 2013, **556**, 65–69.

92 B. Xue, D. B. Harwood, J. L. Chen and J. I. Siepmann, Monte Carlo simulations of fluid phase equilibria and interfacial properties for water/alkane mixtures: An assessment of nonpolarizable water models and of departures from the Lorentz–Berthelot combining rules, *J. Chem. Eng. Data*, 2018, **63**, 4256–4268.

93 A. Mączyński, B. Wiśniewska-Gocłowska and M. Góral, Recommended liquid–liquid equilibrium data. Part 1. Binary alkane–water systems, *J. Phys. Chem. Ref. Data*, 2004, **33**, 549–577.

94 A. Buckingham and R.-L. Disch, The quadrupole moment of the carbon dioxide molecule, *Proc. R. Soc. London, Ser. A*, 1963, **273**, 275–289.

95 Z. Mester and A. Z. Panagiotopoulos, Mean ionic activity coefficients in aqueous NaCl solutions from molecular dynamics simulations, *J. Chem. Phys.*, 2015, **142**, 044507.